Viral Quantitative Capillary Electrophoresis for Counting Intact Viruses

ARTICLE *in* ANALYTICAL CHEMISTRY · JUNE 2011

Impact Factor: 5.64 · DOI: 10.1021/ac201006u · Source: PubMed

5 AUTHORS, INCLUDING:

Gleb G Mironov
University of Ottawa
14 PUBLICATIONS **67** CITATIONS
SEE PROFILE

Rachel Ozer
Royal Ottawa Mental Health Centre
7 PUBLICATIONS **466** CITATIONS
SEE PROFILE

John Bell
The Ottawa Hospital
225 PUBLICATIONS **11,233** CITATIONS
SEE PROFILE

Maxim V Berezovski
University of Ottawa
75 PUBLICATIONS **2,020** CITATIONS
SEE PROFILE

analytical chemistry

ARTICLE

pubs.acs.org/ac

Viral Quantitative Capillary Electrophoresis for Counting Intact Viruses

Gleb G. Mironov,[†] Alexey V. Chechik,[†] Rachel Ozer,[‡,∥] John C. Bell,[‡,§,∥] and Maxim V. Berezovski[*,†]

[†]Department of Chemistry, University of Ottawa, 10 Marie Curie, Ottawa, Ontario K1N 6N5 Canada

[‡]Centre for Cancer Therapeutics, Ottawa Hospital Research Institute, 451 Smyth Road, Ottawa, Ontario K1H 8M5 Canada

[§]Department of Biochemistry, Microbiology and Immunology, University of Ottawa, 451 Smyth Road, Ottawa, Ontario K1H 8M5 Canada

[∥]Jennerex Incorporated, 201 Mission Street, San Francisco, California, United States

Supporting Information

ABSTRACT: The quantification of a virus plays an important role in vaccine development, clinical diagnostics, and environmental contamination assays. In all these cases, it is essential to calculate the concentration or number of intact virus particles (ivp) and estimate the degree of degradation and contamination of virus samples. In this work, we propose a cost-efficient, robust method for the quantification and characterization of intact viruses based on capillary zone electrophoresis. This separation method is demonstrated on vaccinia virus (VV) with oncolytic properties. After virus sample preparation, the solution contains intact VV as well as broken viruses and residual DNA from the host cell used for preparation. Regulatory requirements limit the amount of the host cell DNA that can be present in vaccines or human therapeutics. We apply capillary electrophoresis to separate intact virus particles and the residual DNA and to measure the level of virus contamination with DNA impurities. Intercalating YOYO-1 dye is used to detect the encapsulated and free DNA by laser-induced fluorescence. After soft lysis of VV with proteinase K, all encapsulated DNA is dissolved to the free DNA. The change in peak areas and a DNA calibration curve help determine the initial concentration of intact viruses. This viral quantitative capillary electrophoresis (Viral qCE) is able to quantify the oncolytic vaccinia virus in the range of 10^6 to 10^{12} ivp/mL.

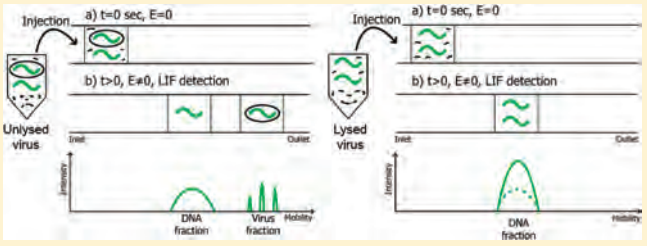

Oncolytic viruses (OVs) promise to improve cancer patient outcomes through their tumor-selective replication and multimodality attack against cancers.[1] The new hope generated by this virus-based technology, including impressive efficacy in animal tumor models, has been somewhat tempered by limited therapeutic activity in the clinic.[2] Human trials have, however, demonstrated that, in general, the OV platform has an exceptional safety profile with much less toxicity, compared to standard forms of cancer therapy like chemo- and radiation therapy.[3] Some viral platforms (namely, vaccinia from Jennerex Biotherapeutics, HSV from Biovex, and Reovirus from Oncolytics Biotech) have entered, or are progressing into, phase III assessment, and thus approval of an OV therapeutic in North America seems to be on the horizon.[4]

Quantification of OVs involves counting the number of viruses in a certain volume to find the virus concentration. It is used in commercial and academic laboratories as well as production situations where the quantity of viruses at various steps is important information. For example, the manufacturing of OVs for cancer therapy, production of viral vaccines, the expression of recombinant proteins using viral vectors and viral antigens all require virus quantification to continually adapt and monitor the process in order to optimize production yields. There are various techniques currently used to quantify viruses in liquid samples such as culture-based and instrumental methods.

The most popular culture-based method is the plaque-forming assay.[5] Viral plaque assays determine the number of plaque-forming units (pfu) in a virus sample, which is one measure of virus quantity. A viral plaque is formed when a virus infects a cell within the fixed cell monolayer. Plaque formation can take 3−14 days, depending on the virus being analyzed. In addition to the plaque assay, there is a 50% tissue culture infective dose ($TCID_{50}$).[6]

There are several traditional instrumental-based methods such as the fluorescent focus assay (FFA),[7] the protein assay,[8] the bicinchoninic acid assay (BCA), and transmission electron microscopy (TEM).[9] Quantitative TEM results will often be higher in number than results from other assays as all particles, regardless of infectivity, are quantified in the reported virus-like particles per milliliter (vlp/mL) result. Quantitative TEM generally works well for virus concentrations greater than 10^6 particles/mL. Because of high instrument cost and the amount of space and

Received: April 19, 2011
Accepted: May 20, 2011
Published: May 21, 2011

support facilities needed, TEM equipment is available in a limited number of facilities.

Modern instrumental methods for virus quantification are relatively new, less time-consuming, and more sensitive like the flow cytometry-based assay,[10] Raman scattering based immune assay,[11] enzyme-linked immunosorbent assay (ELISA),[12] and quantitative polymerase chain reaction (qPCR).[13] qPCR utilizes polymerase chain reaction chemistry to amplify viral DNA or RNA to produce high enough concentrations for detection and quantification by fluorescence. In general, qPCR relies on serial dilutions of standards of known concentration being analyzed in parallel with the unknown samples for calibration and reference. Since PCR amplifies all target nucleic acids, whether from an intact virion or free nucleic acids in solution, qPCR results (expressed in terms of genome copies/mL) are likely to be higher in quantity than viral plaque assay and TEM results.

Viral preparations are also contaminated with DNA from the host cells used to produce the virus. This material is a process impurity in vaccine or therapeutic production and is subject to regulatory limits. The guidance from the World Health Organization is that vaccines should contain less than 10 ng of residual host cell DNA per human dose.[14]

In this work, we introduce a novel method called viral quantitative capillary electrophoresis (Viral qCE). It is a separation-based technique that is able to discriminate between intact virus particles (ivp) and residual DNA with high resolution and sensitivity. Viral qCE is suitable to quantify viruses in the wide dynamic range from 10^6 to 10^{12} ivp/mL. All measurements are performed by a commercial capillary electrophoresis instrument with laser-induced fluorescent detection (CE-LIF) without modifications, suggesting that Viral qCE can be immediately and widely practiced in academic and industrial laboratories.

In our experiments we used the JX-594 strain of vaccinia virus (VV). It is a member of the poxvirus family, and has a large linear double-stranded DNA (dsDNA) genome of approximately 200 kbp in length that encodes ~250 genes. The dimensions of the virion are roughly $360 \times 270 \times 250$ nm^3, with a mass of 5−10 fg. It has several attributes that make it particularly well-suited as an anticancer therapeutic.[15] JX-594 is a virus with a modification of the viral thymidine kinase gene and expression of the immunostimulatory cytokine, GM-CSF (granulocyte macrophage colony-stimulating factor). JX-594 exploits a specific genetic feature in cancer cells to become activated and lyse the cells, including the EGFR-ras signaling pathway, the cell cycle activation, and the loss of cellular interferon defenses. JX-594 is designed to attack cancer through three diverse mechanisms of action: (1) the lysis of cancer cells through viral replication, (2) the reduction of the blood supply to tumors through vascular targeting and destruction, and (3) the stimulation of the body's immune response against cancer cells.

RESULTS AND DISCUSSION

Viral qCE Analysis. The principle of Viral qCE is shown in Figure 1. Briefly, after virus production and storage, the viral sample contains intact viral particles, as well as degraded ones with realized viral DNA, and residual host cell DNA. When the mixture of the virus particles and the free DNA is injected and separated by capillary electrophoresis, two distinctive zones are observed (Figure 1, top). The fast-moving zone contains intact virus particles and is observed as a group of narrow peaks. The slow-moving zone represents the free DNA visible as a wide peak.

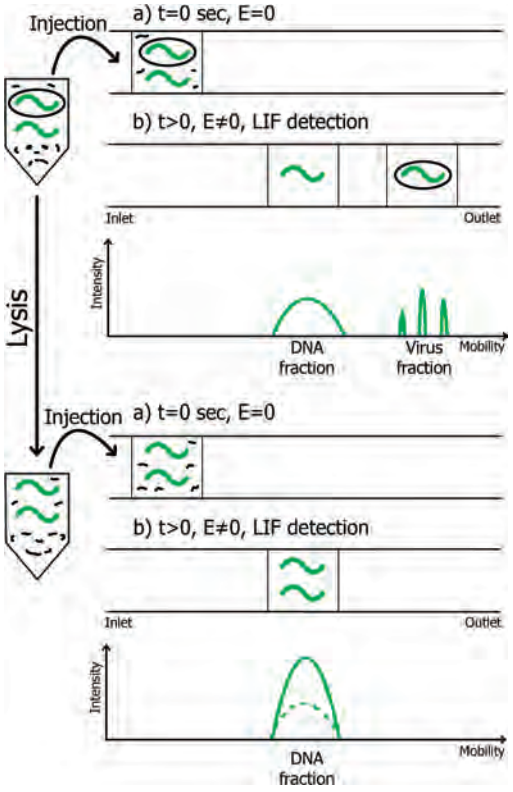

Figure 1. Schematic of diagram of Viral qCE analysis. A mixture of intact virus particles with encapsulated DNA (a green curve in an oval) and the free contaminated DNA (a green curve without an oval) is injected into the capillary as a short plug. When an electric field is applied ($E > 0$ V/cm), viruses and the free DNA are separated into two fractions. After lysis, the virus fraction disappears and the free DNA peak increases. The gain shows the amount of encapsulated DNA before lysis and is used to count intact virus particles. DNA is stained with YOYO-1 dye.

The slow mobility of the free DNA is explained by the multiple negative charges of phosphate groups. After virus lysis by heat or proteases, the fast-moving zone disappears and the slow-moving zone of free DNA becomes more intense (Figure 1, bottom). The gain in peak intensity is due to the DNA release from virus particles, so it can be used to calculate the concentration of the intact particles in the original samples before lysis.

In our experiments we applied YOYO-1 intercalating dye to detect encapsulated DNA and free DNA. YOYO-1 stain shows over a 1000-fold increase in its green fluorescence when bound to dsDNA.[16] YOYO-1 stained the free and encapsulated DNA as seen on the electropherogram at Figure 2B. An anti-VV antibody stained only virus peaks. It helped verify the position of VV peaks during CE analysis (Figure 2C). Virus particles were degraded using proteinase K at 37 °C for 2 h. The moderate heating accelerated proteolysis and prevented DNA denaturation. After the lysis step all viral DNA was released into solution. This was confirmed by the disappearance of the viral particle peaks and the increase of the free DNA peak (Figure 2B). To be certain that VV and YOYO-1 did not have autofluorescence, we tested YOYO-1 only and VV without YOYO-1 in CE (Figure 2A).

Quantitation of Virus Samples with CE. Calculation of the virus concentration was performed in three steps. First, the contamination level (CL) of VV was calculated as

$$\mathrm{CL} = A_0/A_{\mathrm{Lysed}} \quad (1)$$

dx.doi.org/10.1021/ac201006u |Anal. Chem. 2011, 83, 5431–5435

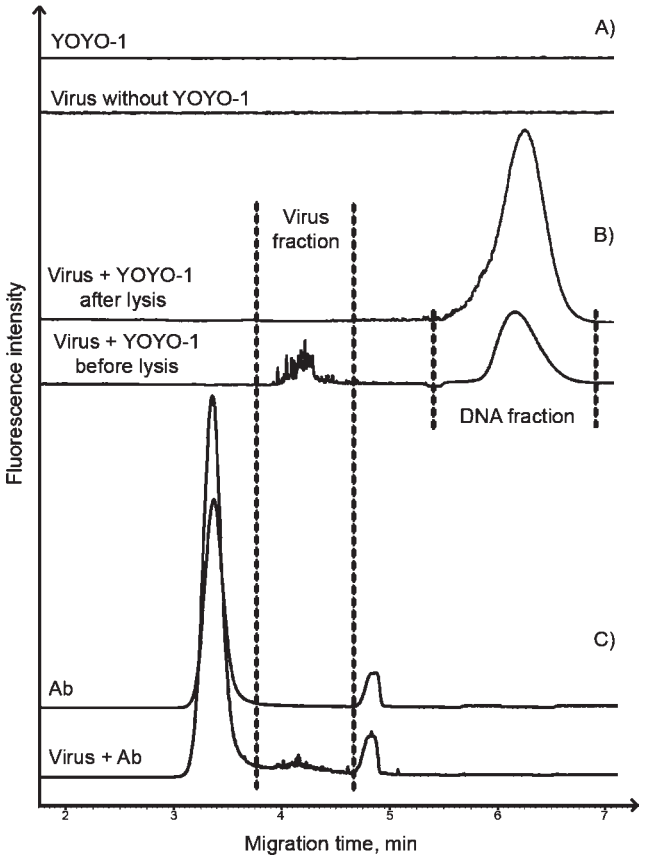

Figure 2. Experimental Viral qCE electropherograms. (A) Control experiments: 1 μM YOYO-1 only (top) and VV without YOYO-1 (bottom). (B) The second lysed VV sample with YOYO-1 (top); the second intact VV sample with YOYO-1 (bottom). (C) A mixture of the primary Ab and the secondary FITC-labeled Ab without VV (top); antibodies with VV (bottom). Peaks stained with Abs and YOYO-1 are shown as the virus fraction. Peaks stained only by YOYO-1 are marked as the DNA fraction. CE separations are performed in a 30 cm long uncoated capillary with 50 mM borax run buffer pH 9.2 under 333 V/cm at 20 °C using LIF detection.

where A_0 and A_{Lysed} are free DNA peak areas before and after lysis, respectively. Second, the concentration of viral DNA in ng/mL was found using calibration curve of serial dilutions of λ phage DNA (λ DNA). The calibration curve was built by plotting fluorescent intensities of YOYO-1-labeled λ DNA samples repeated three times versus their concentrations in ng/mL (Figure 3). The relationship between fluorescent intensity and λ DNA concentration is defined by the equation S3 in the Supporting Information. Practically, serial dilutions of λ DNA (48502 bp) with YOYO-1 were pushed through a capillary by pressure as a continuous flow and their fluorescence intensities were measured. Thereafter, a sample of the lysed virus with YOYO-1 was moved through the capillary the same way as λ DNA and its fluorescence intensity was measured and compared with the standards. In the last step, the concentration of intact virus particles [VV] in ivp/mL was calculated:

$$[\mathrm{VV}] = \frac{(1 - \mathrm{CL})N_A[\lambda\mathrm{DNA}]}{(10^9)(\mathrm{Mr(VV)})} \qquad (2)$$

where [λ DNA] is the concentration of λ DNA in ng/mL found from the calibration curve for the lysed VV sample. N_A is the

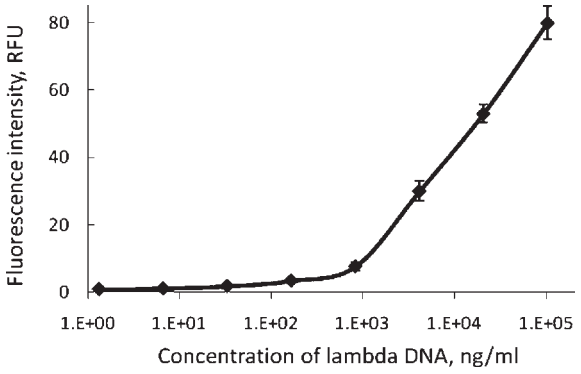

Figure 3. Calibration curve of YOYO-1-stained λ DNA standards for finding viral DNA concentration after lysis. A solution of 1 μM YOYO-1 was used for DNA staining.

Avogadro constant (6.022×10^{23} mol^{-1}) and Mr(VV) is the molar mass of the viral DNA in g/mol and equals 135×10^6 g/mol for VV. Spiking the actual viral sample with known amounts of λ DNA and generating the standard curve in the presence of viral DNA can be useful to eliminate the influence of sample media. We did not notice a big difference with the spiking method, because our VV samples were diluted in 10 mM borax buffer before CE analysis.

Three samples of VV were studied. The first contained 2 month old VV, the second sample had VV from a different batch that underwent 20 freeze/thaw cycles, and the third sample contained the freshly prepared virus. The degradation and concentration was calculated to be 2% and $(4.5 \pm 0.4) \times 10^9$ ivp/mL for the first sample, 30% and $(7.7 \pm 1.4) \times 10^9$ ivp/mL for the second, and 10% and $(1.6 \pm 0.3) \times 10^{10}$ ivp/mL for the third sample, respectively. The second VV sample had the significant amount of degraded or contaminated DNA, as the intensive zone of free DNA was observed in Figure 2B. The additional Viral qCE electropherograms are shown in Supporting Information Figure S1 for different virus concentrations.

Different methods (temperature, sonication, and SDS) of virus lysis were also evaluated. We found that temperature denaturation of VV had a big disadvantage—it melted big viral DNA and prevented YOYO-1 intercalation making the assay irreproducible. Sonication did not give consistent results as well. The lysis with SDS worked relatively well with 5% SDS solution and consequent 20 times dilution of the virus lysate. High concentration of SDS decreases binding of YOYO-1 to DNA. The most stable results were obtained using proteinase K. It is a broad-spectrum serine protease. The predominant site of cleavage is the peptide bond adjacent to the carboxyl group of aliphatic and aromatic amino acids with blocked alpha amino groups. Adding proteinase K to nucleic acid preparations rapidly inactivates nucleases that might otherwise degrade the DNA during sample preparation.[17]

We should consider that differences in sample constituents of λ DNA and VV could influence on the precise quantification of the virus DNA due to various behaviors of the intercalating YOYO dye in different conditions. To reduce this effect all samples and standards were prepared and diluted in the same buffer and analyzed in the same run buffer. We also applied an excess of the dye (1 μM) to saturate and keep constant the dye/base pair ratio. We suggest that DNA isolated from a target virus can be used for making a calibration curve. The efficiency of the dye intercalation and proteinase digestion was tested on

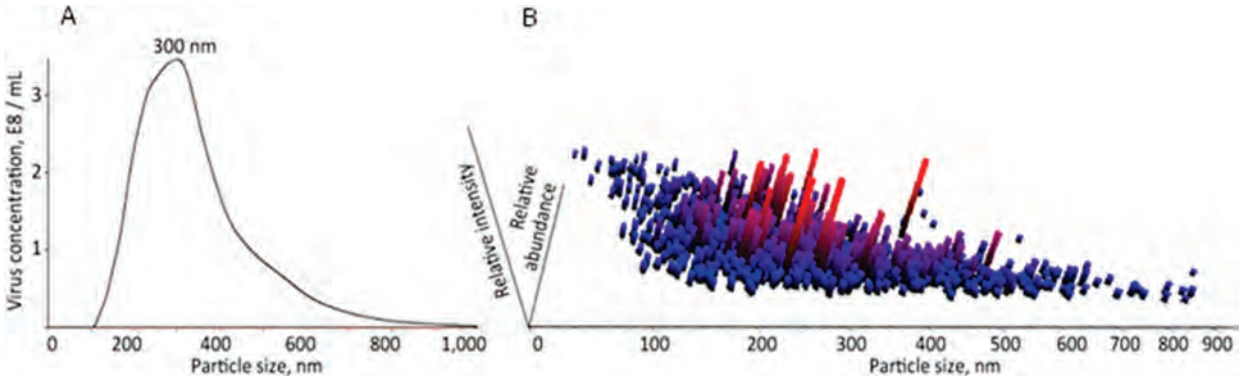

Figure 4. Size distribution from NTA measurement (panel A) and 3D graph (size vs intensity vs abundance; panel B) of vaccinia virus.

replicate analysis of virus samples before and after lysis (Supporting Information Figure S2).

Quantitation of Viruses with NanoSight. To verify the quantitation of intact viral particles by Viral qCE, an additional technique called nanoparticle tracking analysis (NTA) and a "NanoSight" instrument were used.[18] The NTA analysis is based on a laser-illuminated microscopy technique. Brownian motion of nanoparticles is analyzed in real time by a charge-coupled device (CCD) camera; each particle is being simultaneously but separately visualized and tracked by a dedicated particle tracking image analysis software. The software is capable of distinguishing bright particles captured by the CCD camera from black background and further tracking them while they are in the focus. The distance run by every single particle over a time period results in the speed value which is reversely proportional to particle size. Depending on side scattering and the speed of the particles' movement it is possible to determine their concentration and size. NanoSight is able to simultaneously visualize and analyze nanoparticles on an individual basis from heterogeneous samples in the size range of 10−1000 nm and the concentration range from 10^7 to 10^9 particles/mL.[19]

We applied the NanoSight instrument to analyze the first (2 month old) sample of VV (Figure 4). Its concentration was measured to be $(2.5 \pm 0.3) \times 10^9$ ivp/mL. As seen in Figure 4A, VV has a wide size distribution with the maximum on 300 nm and a right shoulder. This maximum value is the average of linear dimensions of a virion ($250 \times 270 \times 360$ nm^3). The right shoulder represents self-aggregation of the virus. Figure 4B shows the distribution of particles by their size, the relative intensity of light scattering, and the abundance (or tracking stability) of the particles. The relative intensity can be used to discriminate virus particles from high-scatter agglomerates (cell debris, denatured viruses, and polymer beads). Contaminated host cell DNA was not detected by the NanoSight due to a very small size (<10 nm).

We confirm three major advantages of Viral qCE. First, it works in a wider dynamic range of virus concentrations from 10^6 to 10^{12} ivp/mL than NanoSight (10^7 to 10^9 ivp/mL). Second, the sample consumption is very low (5−40 μL for CE vs 300−1000 μL for NanoSight). The third benefit is the ability to calculate the level of virus contamination by denatured viral DNA or residual cellular DNA impurities.

CONCLUSION

In this article, we demonstrated a CE-based method for reliable quantification of intact virus particles. Viral qCE can be done in 5−15 min and requires minimal skills for the optimization of CE separation. Viral qCE enables partitioning of intact viral particles and free DNA and measures an exact intact particle concentration and host cell DNA impurity contamination of viral samples. CE with LIF detection is very sensitive and accurate, and it has a wide dynamic range of virus quantification. It can also distinguish non-DNA impurities and exclude them from calculations. Viral qCE gives the possibility of live monitoring heat-induced aggregation, providing information about the aggregation kinetics. We foresee that the presented method can be applied for quality control in oncolytic viruses and vaccine productions.

MATERIALS AND METHODS

Chemicals and Materials. Vaccinia virus samples and a purified polyclonal rabbit antivaccinia primary antibody were provided by Jennerex Inc. (Ottawa, ON, Canada). Chemicals were purchased from the following companies: λ DNA (cat. no. M6201, Biomatik Corporation, Canada), sodium borate decahydrate (cat. no. SX0355-1, EMD Chemicals, U.S.A.), YOYO-1 dye (cat. no. N7565, Invitrogen, U.S.A.), proteinase K (cat. no. AM2546, Ambion, U.S.A.), FITC-labeled goat antirabbit antibody (cat. no. A11009, Invitrogen, U.S.A.). The bare silica capillary with an o.d. of 365 μm and an i.d. of 75 μm was purchased from Polymicro Technologies (cat. no. TSP075375, Phoenix, AZ, U.S.A.). All buffers were made using Milli-Q-quality deionized water and filtered through a 0.22 μm filter.

Preparation of Lysed Virus and DNA Standards. Proteinase K solution (1 μL of 20 mg/mL) was added to 19 μL of virus or λ DNA solution with subsequent heating at 37 °C for 2 h. The control of nonlysed samples was prepared identically, but 1 μL of 10 mM borax buffer was used instead of proteinase K.

Standards of λ DNA were prepared by the serial dilution (5, 5^2, 5^3, 5^4, 5^5, 5^6, 5^7, and 5^8 times) of 500 μg/mL stock solution in 10 mM borax buffer. Working samples of VV were prepared from the stock solution of the virus by 5, 5^2, 5^3, 5^4 and 5^5 times stepwise dilution in 10 mM borax buffer. An amount of 0.88 μL of 10 μM YOYO-1 was added to 8 μL of each standard solution of λ DNA and working solution of the virus.

Capillary Electrophoresis. Capillary electrophoresis analyses were performed using a PA800+ pharmaceutical analysis capillary electrophoresis system (Beckman Coulter, Brea, CA, U.S.A.) with LIF detection. Fluorescence was excited with a 488 nm line of a solid-state laser and detected at 520 ± 10 nm. Separations were carried out using a bare fused-silica capillary of 30 cm in total length and 20.5 cm from an injection point to a detection

window. Hydrodynamic injection of a sample (45 nL) was made by a pressure pulse of 0.5 psi for 5 s for the CE separation. The total fluorescence of the sample was measured by pushing it through the capillary as a continues plug with pressure of 5 psi for 3 min. The CE separations were conducted by applying a voltage of 10 kV (an electric field of 333 V/cm) when a positive charge is at the inlet and the ground at the outlet. The temperature of the capillary and samples was kept constant at 20 °C. The output data was fluorescence intensity in the detection point, as a function of time passed since the application of the electric field. Data were collected and analyzed using 32 Karat version 8.0 software. The run buffer was 50 mM sodium tetraborate (borax) at pH 9.2. At the start of each run, prior to injection, the capillary was rinsed with 0.1 M HCl for 2 min, 0.1 M NaOH for 2 min, deionized water for 2 min, and the run buffer for 4 min.

NanoSight Measurements. Different concentrations (from 10^7 to 10^9 vp/mL) of VV in PBS were measured using a NanoSight LM10 system (NanoSight Ltd., U.K.). The software used for capturing and analyzing the data was the NTA 2.0. The particle numbers were counted by their scattered light spots which could be identified clearly on the video image. The mean particle number per frame was counted from 1800 frames of the videos from five measurements of each sample. The video was recorded for 60 s at 30 frames/s for each measurement. NanoSight was preliminary calibrated with 100, 200, and 400 nm polystyrene microspheres in concentration between 10^7 and 10^9 beads/mL (Nanosphere from Thermo Scientific, Fremont, CA). Three measurements of the same sample were performed for all polystyrene beads and six measurements for virus samples. The relative average error of these measurements was about 12%.

■ ASSOCIATED CONTENT

Supporting Information. Additional information as noted in text. This material is available free of charge via the Internet at http://pubs.acs.org.

■ AUTHOR INFORMATION

Corresponding Author
*E-mail: maxim.berezovski@uottawa.ca.

■ ACKNOWLEDGMENT

This work was supported by the Natural Sciences and Engineering Research Council of Canada's Engage Grant and Ottawa Technology Transfer Network's Proof of Principle Fund (OTTN-PoP). The authors also thank Dr. Victor Okhonin, Ms. Jennifer Logie, and Ms. Ekaterina Berezovskaia for critical reviews and valuable suggestions.

■ REFERENCES

(1) Parato, K. A.; Senger, D.; Forsyth, P. A.; Bell, J. C. *Nat. Rev. Cancer* **2005**, *5*, 965–976.
(2) Aghi, M.; Martuza, R. L. *Oncogene* **2005**, *24*, 7802–7816.
(3) Liu, T. C.; Hwang, T.; Park, B. H.; Bell, J.; Kirn, D. H. *Mol. Ther.* **2008**, *16*, 1637–1642.
(4) Park, B. H.; Hwang, T.; Liu, T. C.; Sze, D. Y.; Kim, J. S.; Kwon, H. C.; Oh, S. Y.; Han, S. Y.; Yoon, J. H.; Hong, S. H.; Moon, A.; Speth, K.; Park, C.; Ahn, Y. J.; Daneshmand, M.; Rhee, B. G.; Pinedo, H. M.; Bell, J. C.; Kirn, D. H. *Lancet Oncol.* **2008**, *9*, 533–542.
(5) Niwa, O.; Decleve, A.; Liberman, M.; Kaplan, H. S. *J. Virol.* **1973**, *12*, 68–73.
(6) Saliba, G. S.; Franklin, S. L.; Jackson, G. G. *J. Clin. Invest.* **1968**, *47*, 1303–1313.
(7) Payne, A. F.; Binduga-Gajewska, I.; Kauffman, E. B.; Kramer, L. D. *J. Virol. Methods* **2006**, *134*, 183–189.
(8) Garrison, A. R.; Alakbarova, S.; Kulesh, D. A.; Shezmukhamedova, D.; Khodjaev, S.; Endy, T. P.; Paragas, J. *Am. J. Trop. Med. Hyg.* **2007**, *77*, 514–520.
(9) Hara, S.; Terauchi, K.; Koike, I. *Appl. Environ. Microbiol.* **1991**, *57*, 2731–2734.
(10) Marie, D.; Brussaard, C. P. D.; Thyrhaug, R.; Bratbak, G.; Vaulot, D. *Appl. Environ. Microbiol.* **1999**, *65*, 45–52.
(11) Driskell, J. D.; Kwarta, K. M.; Lipert, R. J.; Porter, M. D.; Neill, J. D.; Ridpath, J. F. *Anal. Chem.* **2005**, *77*, 6147–6154.
(12) Crowther, J. R.; Reckziegel, P. O.; Prado, J. A. *Vaccine* **1995**, *13*, 1064–1075.
(13) McQuaig, S. M.; Scott, T. M.; Lukasik, J. O.; Paul, J. H.; Harwood, V. J. *Appl. Environ. Microbiol.* **2009**, *75*, 3379–3388.
(14) van Aken, W. G.; Calam, D.; Pewsey, M.; Castillo, A. C.; Dobbelaer, R.; Fuchs, F.; Homma, A.; Kurata, T.; Medunitsin, N. V.; Ofosu, F. In *WHO Expert Committee on Biological Standardization: Fifty-Third Report*; World Health Organization: Geneva, Switzerland, 2004.
(15) Jacobs, B. L.; Langland, J. O.; Kibler, K. V.; Denzler, K. L.; White, S. D.; Holechek, S. A.; Wong, S.; Huynh, T.; Baskin, C. R. *Antiviral Res.* **2009**, *84*, 1–13.
(16) Auzanneau, I.; Barreau, C.; Salome, L. *C. R. Acad. Sci., Ser. III* **1993**, *316*, 459–462.
(17) Hilz, H.; Wiegers, U.; Adamietz, P. *Eur. J. Biochem.* **1975**, *56*, 103–108.
(18) Filipe, V.; Hawe, A.; Jiskoot, W. *Pharm. Res.* **2010**, *27*, 796–810.
(19) Du, S.; Kendall, K.; Morris, S.; Sweet, C. *J. Chem. Technol. Biotechnol.* **2010**, *85*, 1223–1228.

SUPPORTING INFORMATION

Viral Quantitative Capillary Electrophoresis (Viral qCE) for Counting Intact Viruses

Gleb G. Mironov[1], Alexey V. Chechik[1], Rachel Ozer[2,4], John C. Bell[2,3,4] and Maxim V. Berezovski[1*]

[1]Department of Chemistry, University of Ottawa, Ottawa, Ontario, Canada; [2]Centre for Cancer Therapeutics, Ottawa Health Research Institute, Ottawa, Ontario, Canada; [3]Department of Biochemistry, Microbiology and Immunology, University of Ottawa, Ottawa, Ontario, Canada; [4]Jennerex Inc., San Francisco, California, USA,

*Correspondence: Maxim V. Berezovski, Department of Chemistry, University of Ottawa, 10 Marie Curie, Ottawa, Ontario K1N 6N5, Canada. E-mail: maxim.berezovski@uottawa.ca

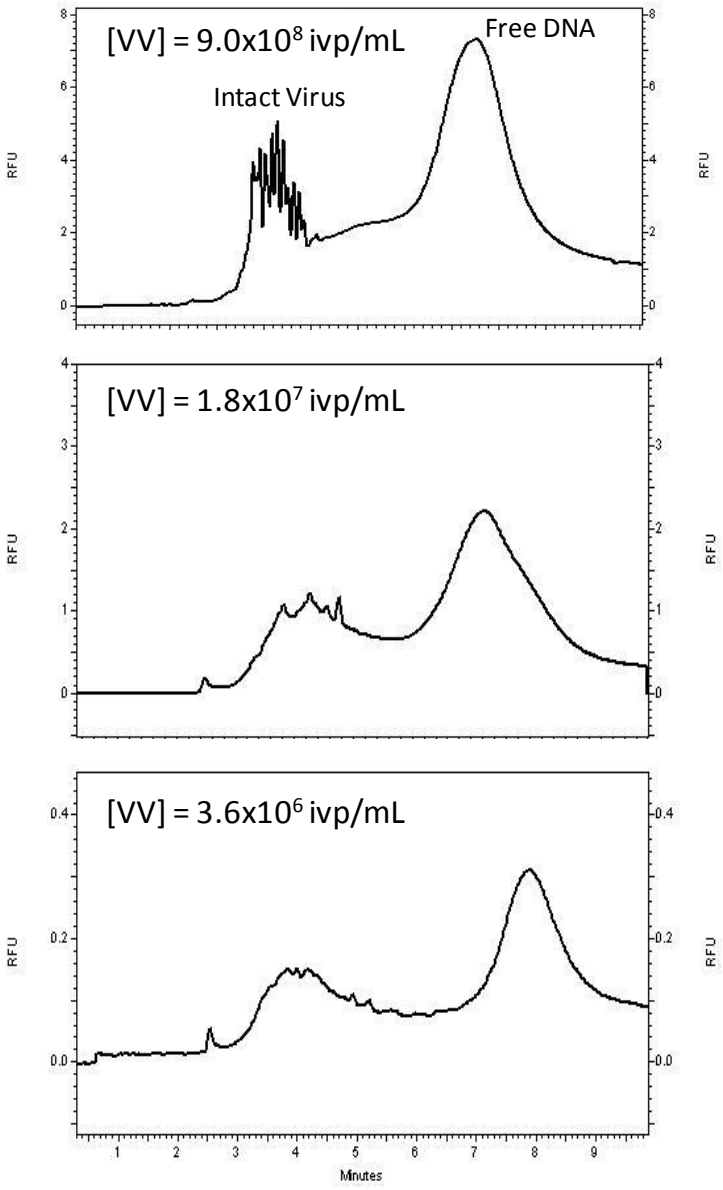

Figure S1. Experimental Viral qCE electropherograms of different Vaccinia Virus (VV) concentrations. VV is stained with 1 μM YOYO-1. CE separations are performed in 50 cm-long uncoated capillary with 50 mM Borax run buffer pH 9.2 under 200 V/cm at 20˚C using LIF detection.

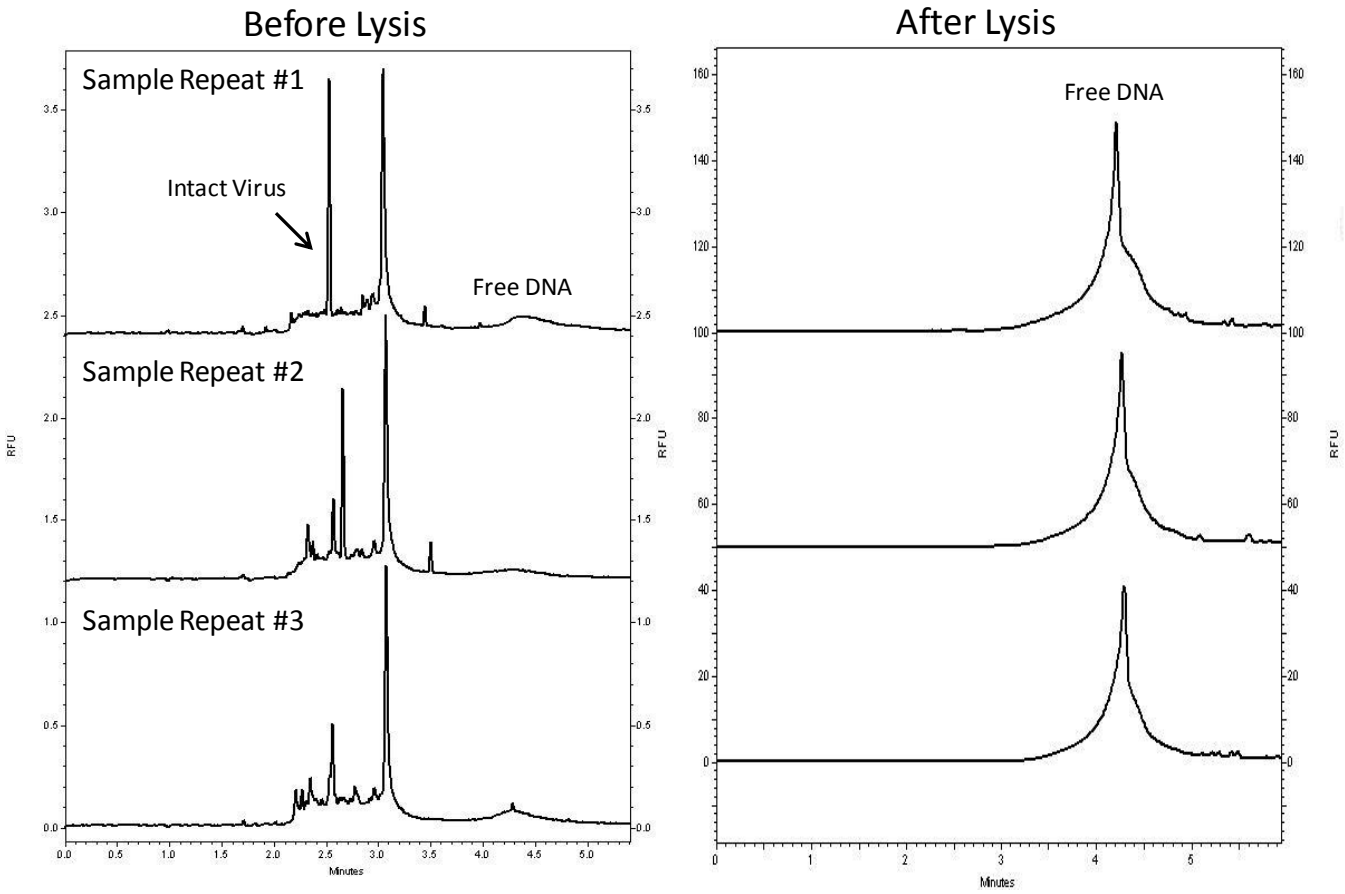

Figure S2. Viral qCE analysis for three replicates of a virus sample before lysis and after lysis with protease K. Stained with 1 μM YOYO-1. CE separations are performed in 30 cm-long uncoated capillary with 50 mM Borax run buffer pH 9.2 under 333 V/cm at 20˚C using LIF detection.

Estimation of Measurement Errors

In Viral qCE, the areas of DNA peaks are measured before and after lysis with relative errors (δ_{rel}^{b}, δ_{rel}^{a}) and defined as $b\left(1\pm\delta_{rel}^{b}\right)$ and $a\left(1\pm\delta_{rel}^{a}\right)$, respectively. The resulting area gain, Δ and the relative measurement error, δ_{rel}^{Δ} can be expressed by the following equation:

$$\Delta\left(1\pm\delta_{rel}^{\Delta}\right)=a\left(1\pm\delta_{rel}^{a}\right)-b\left(1\pm\delta_{rel}^{b}\right)=\left(a-b\right)\pm\sqrt{\left(a\delta_{rel}^{a}\right)^{2}+\left(b\delta_{rel}^{b}\right)^{2}}$$

$$\delta_{rel}^{\Delta}=\sqrt{\left(a\delta_{rel}^{a}\right)^{2}+\left(b\delta_{rel}^{b}\right)^{2}}\Big/\left(a-b\right) \qquad \text{(S1)}$$

Using a simplifying assumption for relative errors, $\delta_{rel}^{b}=\delta_{rel}^{a}=\delta_{rel}$, the relative error of the gain can be found as:

$$\delta_{rel}^{\Delta}=\frac{\delta_{rel}}{a-b}\sqrt{a^{2}+b^{2}} \qquad \text{(S2)}$$

In the case when the peak of free DNA before lysis is small ($b \ll a$), the relative error for the gain is similar with relative errors of all measurements (for example, for $b=a/10$, $\delta_{rel}^{\Delta} \approx 1.1\delta_{rel}$). In the situation when the gain is small ($b \sim a$), the relative error for the gain is increasing dramatically (for $b=0.9a$, $\delta_{rel}^{\Delta} \approx 13.5\delta_{rel}$).

Linearity of Calibration Curve

The relationship between fluorescent intensity, *i*, and concentration of lambda DNA on the calibration curve at Figure 3 can be modelled by the following equation.

$$[\lambda\mathrm{DNA}] = 8.778 \cdot 10^{-8} \cdot i + 1.797 \cdot 10^{-12} \cdot i^{4.158} - 7.717 \cdot 10^{-08} \qquad \text{(S3)}$$

There are two intervals where the dependence can be linearized: (i) the low intensity interval ($0< i <10$), where the dependence of [DNA] is a linear function of the intensity, and (ii) the high intensity interval ($30< i <100$), where the dependence for the logarithm of DNA concentration is a linear function of the logarithm of the intensity. The intermediate case ($10< i <30$) can be better described by the full equation (S3).